Ninth International Conference on CFD in the Minerals and Process Industries
CSIRO, Melbourne, Australia
10-12 December 2012

VALIDATION OF CFD MODELS USING FLOW3D FOR A SUBMERGED LIQUID JET

Nurul HASAN*

CEO, Don Computing, 39/385 Bourke Street, Melbourne, VIC 3000 Australia
drnhasan@doncomputing.com

ABSTRACT

This paper presents a step by step verification and validation process of a vertical round submerged jet into a cylindrical bath. Taking advantage of the axi-symmetric domain, Navier-Stokes equation of primary is solved by finite volume method (FVM) using commercial computational fluid dynamics, CFD (Flow-3D) software. For verification and to minimise the computational error, step by step grid independence tests were performed. For validation, experimental data was produced using laser Doppler velocimetry (LDV). Among the turbulence model, RNG was found to predict the flow behaviour better than k - ε models.

NOMENCLATURE

- p Pressure
- $\mathbf{u}$ Velocity
- ρ Density
- μ Dynamic viscosity
- d_0 Diameter of the nozzle
- D_c Diameter of the cylinder
- H_l Height of liquid
- H_c Height of the cylinder
- h Submerged depth

INTRODUCTION

It is absolute necessary to perform strategic verification and validation for CFD results to be trustworthy. To produce experimental data and analysing the data, there are difficulties; on the other hand there are limitations of the turbulence models of CFD.

For a liquid jet vertically flowing downwards to a cylindrical receiving bath, the fluid decelerates and spreads while the surrounded liquid is entrained. It is a usual practice in the experiments to use honeycomb (Strykowski and Niccum, 1992) before delivering the jet and to smooth the turbulence intensity and to straighten the nozzle inlet piping to suppress possible swirl (Yang et al., 2000).

The CFD validation studies performed previously in this area involves mainly the computational centre line velocity comparision against the experimental data, e.g., (Bayly et al., 1992). Due to large number of cases studied, Devahastin and Mujumdar (Devahastin and Mujumdar, 2002) could not check the grid independence for each study for the numerical study of flow and mixing characteristics of laminar confined impinging streams. Rather, the grid doubling is performed for the highest Reynolds number and used that grid size for low Reynolds number as well as suggested by others (Hosseinalipour and Mujumdar, 1997).

It has been a tradition to compare the computational results with the experimental results and to stop refinement as the computational results agree with the experimental results, which is not a fair practice. It may be the case that the researchers are using more or less mesh than it requires. For example, Wilson and Imber (Wilson and Imber, 2001) studied a computational model of a rectangular jet ($\mathrm{Re}_j = \dfrac{d_0 u_0 \rho_l}{\mu_l}$ =1.49X10^5) with aspect ratio 10, issuing into a quiescent environment as a free jet and validated the computational results against experimental data with good agreement. The readers may want to know what would happen, if the grid of Wilson and Imber (Wilson and Imber, 2001) were refined further.

This paper is designed as follows: section next defines the computational model and boundary conditions, and then results with verification and validation. The conclusions are added at the end.

MODEL & BOUNDARY CONDTIONS

The continuity eq. (1), and momentum eq. (2), are solved numerically by commercial software, and called Flow-3D for three different applications.

$$\nabla \cdot (\mathbf{u}) = 0 \tag{1}$$

$$\frac{\partial \rho \mathbf{u}}{\partial t} + \nabla \cdot (\rho \mathbf{u}\mathbf{u}) = -\nabla p + \nabla . \mu \nabla \mathbf{u} \tag{2}$$

The computational model is shown in **Figure 1** is for a water submerged jet nozzle on a cylindrical receiving bath. This experiment was performed at the University of Newcastle, Australia. There was significant change on the free surface, so in CFD, the free surface was considered as wall. An inlet boundary condition was used at nozzle pipe inlet for a 12 l/m flow rate. The inlet pipe in the computational model has a length of 200-400 mm and 9.6 mm diameter (same as experiment). The receiving cylinder has 500 mm length and 90 mm dia. The inlet pipe has 145 mm inside the receiving cylinder. The exit pipe was 200 mm in length and 12 mm diameter. The flow rate of the liquid inlet and outlet are the same and there is no mass accumulation in the cylindrical bath for steady state calculation. So, computationally, there is no accumulation of liquid in the receiving cylindrical bath, because a controlled outlet of liquid in the centre of the bottom of cylindrical bath that is set to have the flow rate as the inlet.

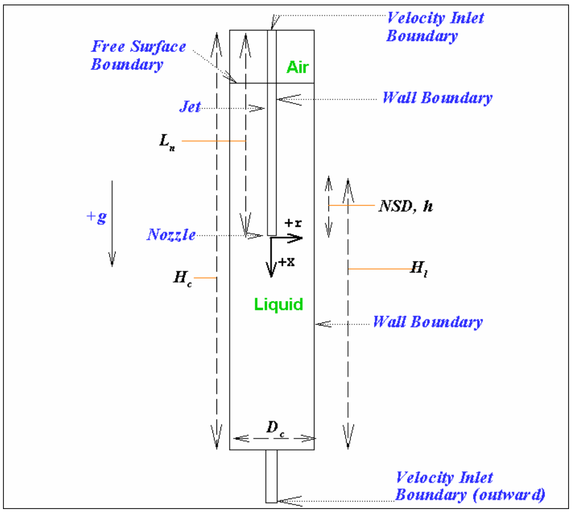

Figure 1: Schematic diagram of computational domain submerged jet case.

Table 1 shows the mesh quality for mesh2, one of the three meshes was tested. A 30 degree 3D domain was developed and symmetry BC was considered on two sides (Figure 2). The meshing method in Flow-3D is different from all other commercial codes. First a solid cylinder was created, and then a hollow space representing the receiving cylinder was subtracted from the first cylinder. On the two sides of the first cylinder, two holes were made to represent the inlet and outlet. Only fluid flow model was considered and in the solid domain there was no simulation. Table 1 shows few important features.

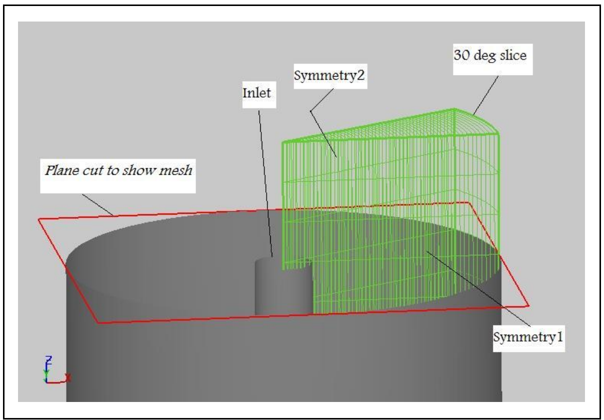

Figure 2: The domain has been cut through to show the 30 slice with mesh along with inlet.

First, all the meshes considered were structured meshes of equal size in one direction. As the total computation time was very small, it was not made an effort to make many blocks and refined the mesh locally. In the axial direction, the mesh size was 0.009 m. In the rotational direction, there was only one mesh (Figure 3) assuming that there is no significant swirling flow. As the mesh size for mesh2 is 0.00045 m in the radial direction and nozzle radius is 0.0048, there were 11 cells along the inlet and 14 cell along the outlet radial direction (mesh2).

Table 1: Summary of Mesh2

r direction: # of real cells=	100
smallest cell =	4.5000E-04
largest cell =	4.5000E-04
maximum cell ratio =	1.0000E+00
y direction: # of real cells=	1
smallest cell =	2.3562E-02
largest cell =	2.3562E-02
maximum cell ratio =	1.0000E+00
z direction: # of real cells=	100
smallest cell =	9.0000E-03
largest cell =	9.0000E-03
maximum cell ratio =	1.0000E+00

The original mesh was considered is mesh1, the details are shown in Table 2. In mesh2, the radial mesh number is doubled (Table 1) keeping the axial refinement the same. In mesh3 (Table 3), the axial mesh is doubled keeping the radial size same as mesh2. Here in all cases, the y direction represents the swirling direction, z as the axial direction and x is the radial direction (Figure 4). In all cases the mesh size was kept consistent in one direction. The other alternative was to make more blocks and control the mesh size.

Table 2: Summary of Mesh1

r direction: # of real cells=	50
smallest cell =	9.0000E-04
largest cell =	9.0000E-04
maximum cell ratio =	1.0000E+00
y direction: # of real cells=	1
smallest cell =	2.3562E-02
largest cell =	2.3562E-02
maximum cell ratio =	1.0000E+00
z direction: # of real cells=	100
smallest cell =	8.5500E-03
largest cell =	8.5500E-03
maximum cell ratio =	1.0000E+00

Table 3: Summary of Mesh3

r direction: # of real cells=	100
smallest cell =	4.5000E-04
largest cell =	4.5000E-04
maximum cell ratio =	1.0000E+00
y direction: # of real cells=	1
smallest cell =	2.3562E-02
largest cell =	2.3562E-02
maximum cell ratio =	1.0000E+00
z direction: # of real cells=	200
smallest cell =	4.2750E-03
largest cell =	4.2750E-03
maximum cell ratio =	1.0000E+00

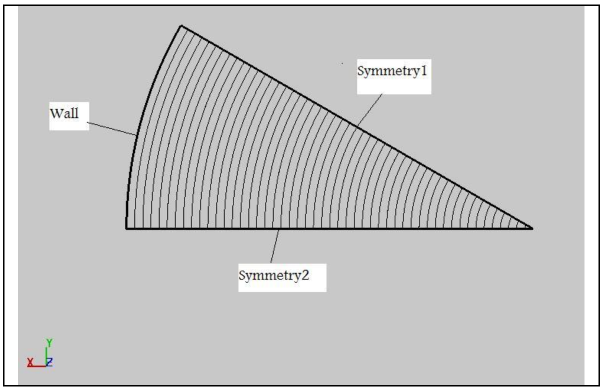

Figure 3: Top view showing mesh along the radial direction with one mesh in radial direction.

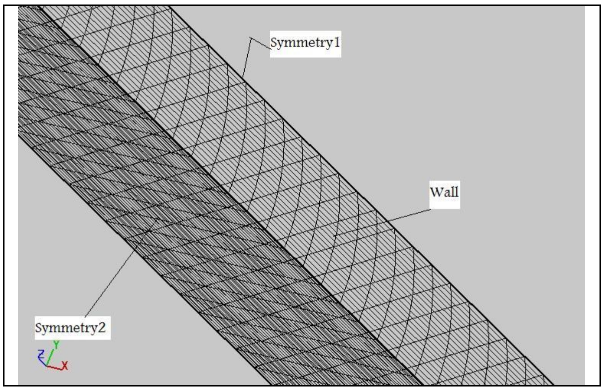

Figure 4: 3D view of the 30 degree mesh with the boundary conditions.

FAVOR is an acronym for Fractional-Area-Volume-Obstacle-Representation is the strong plus of Flow-3D (Flow3d, 2012). It was originally developed for defining obstacles of general shape within a grid composed of rectangular brick elements (Hirt and Sicilian, 1985). These fractions are then incorporated into the finite-volume equations of motion. The strength of the FAVOR method is the modeling flexibility it offers. For heat transfer between fluids and solids, the FAVOR method should give high solution accuracy by providing a good approximation of the areas of the fluid/obstacle interface within each brick element. In the FAVOR method, a surface is allowed to cut through an element compared to the BFC (body fitted coordinate). The location of solid surface in FAVOR is recorded by the fractional face areas and fractional volume of the element covered by the solid. This is great advances of meshing for complex geometries, however, lots of blocks are needed to resolve flow around a boundary.

RESULTS

Figure 5 shows the velocity vector for k - ε model along with mesh for the 12 l/m flow rate. Nearly up to 3 diameter of the cylinder from the exit of the nozzle, there is significant velocity gradient. The radial influence of submerged jet is maximum at twice the diameter of the cylinder from the exit of the nozzle to cylinder. This kind of flow behaviour has been reported by the experiments. The next figure (Figure 6) will show a better comparison compared to experimental data.

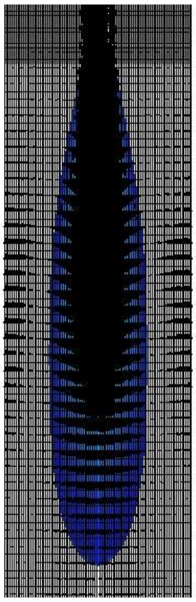

Figure 5: On mesh 1, the velocity vector showing zone where there is significant velocity gradient (showing mesh as well.

Figure 6 (left) shows velocity magnitude for all three meshes considered for RNG models. The experimental velocity magnitude (left of Figure 6) is the square root of the sum of the squares of the three velocity components. Apparently, the mesh is fine enough for velocity prediction for all three meshes. However, Figure 6 (right) shows that the mesh is sensitive around 0.6 to 0.8 from the exit. So even the mesh is good enough for velocity magnitude, it is not good enough for turbulence predictions. In all cases, the CFD predictions were lower than the experimental data, partially because the swirling flow is not predicted in CFD assuming there is no swirl.

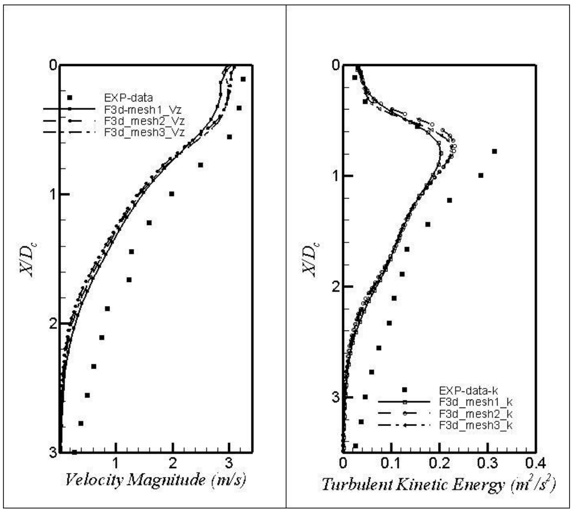

Figure 6: centre line velocity magnitude (m/s) and turbulent kinetic energy for four different meshes [V_q =12 litre/min,].

Figure 7 shows the predictions for two turbulence models: RNG and k - ε . Left figure shows the centre line velocity and right size shows the k at the centre line. Beyond the distance of one unit from the nozzle, the k - ε predicts higher centre line velocity compared to *RNG*. On the other hand, between the distance 0.4 to 0.8, *RNG* predicts higher k compared to k - ε model and the opposite occurs between 2-3.

As shown in Figure 6, above X / D_c =1.0, both k - ε and RNG fails to predict the k . The experimental turbulent kinetic energy is calculated as $\frac{1}{2}\left(\sigma^2{}_x + \sigma^2{}_y + \sigma^2{}_z\right)$, where σ_i is the root mean square velocity *fluctuation* components. Next to the nozzle exit, higher gradient of velocity (left of Figure 6) exists, which results in high turbulence production as can be seen from Figure 6 (right).

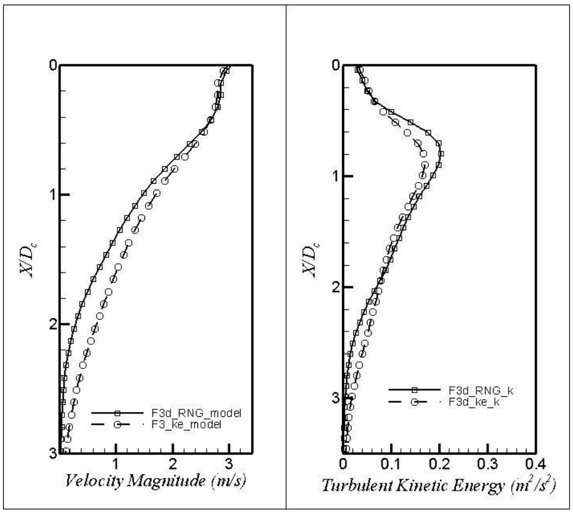

Figure 7: Velocity magnitude and turbulent kinetic energy for two different turbulent models.

There are controversies on how the experimental turbulent kinetic energy is calculated. The experimental σ_y was not same as σ_x which states the non isentropic nature, especially about one unit length after the nozzle exit.

CONCLUSION

Taking an advantage of axi-symmetric nature, the fluid flow as investigated shows that CFD prediction of the fluid through a submerged liquid jet can be predicted reasonably well. RNG offers better results compared to k - ε in terms of velocity and turbulent parameters predictions. The experimental turbulent kinetic parameter is a controversial issue. The major differences may be because in CFD, the swirling flow is not predicted. However, in most cases, the swirling nature in not completely reported by the experimentalists.

There are few reasons why there were discrepancies in predictions. The 1st reason for discrepancy is probably because k - ε and RNG is not very accurate in predicting sharp gradient in velocity. The 2nd reason for discrepancy is because flow exit at the bottom in the experiment is not strictly constant, whereas the exit in the CFD simulations used is very constant. Next, LES will be used for this submerged jet flow.

ACKNOWLEDGMENT

This work was supported by grants ARC, Australia. Part of the computing time was provided by the VISLAB (the University of Sydney), CANCES (the University of New South Wales). The authors also would like to thank Professor Clive Fletcher (the University of New South Wales), Prof Geoff Evans (the University of Newcastle), Dr. Qinglin He (the Centre for Multiphase Flow) and the reviewers for helpful comments and suggestions. The experimental data is old (12 years old), however, the CFD results are recently produced.

REFERENCES

BAYLY, A. E., RIELLY, C. D., EVANS, G. M., AND HAZELL, M., (1992), "*The Rate of Expansion of A Confined, Submerged Jet*". *20th Australasian Chemical Engineering Conference, Canberra*.

DEVAHASTIN, S., AND MUJUMDAR, A. S., (2002), "*A numerical study of flow and mixing characteristics of laminar confined impinging streams"*. *Chemical Engineering Journal (Amsterdam, Netherlands)*, **85,** 215-223.

Flow3d, (2012), "*FLOW-3D: Computational Modeling Power for Scientists and Engineers*". Flow Science, Inc. report, FSI-87-00-01.

HIRT, C. W., AND NICHOLS, B. D., (1981), "*Volume of fluid (VOF) method for the dynamics of free boundaries". Journal of computational physics*, **39,** 201-225.

HIRT, C. W., AND SICILIAN, J. M., (1985), "*A porosity technique for the definition of obstacles in rectangular cell meshes*".

HOSSEINALIPOUR, S. M., AND MUJUMDAR, A. S., (1997), "*Flow and thermal characteristics of steady two dimensional confined laminar opposing jets. Part II. Unequal jets". International Communications in Heat and Mass Transfer*, **24,** 39-50.

STRYKOWSKI, P. J., AND NICCUM, D. L., (1992), "*The influence of velocity and density ratio on the dynamics of spatially developing mixing layers". Physics of Fluids A: Fluid Dynamics*, **4,** 770-781.

WILSON, W. M., AND IMBER, R. D., (2001), "*CFD Analysis of Compact, High Aspect Ratio Ejectors*". *Proceedings of ASME FEDSM*.

YANG, Y., CROWE, C. T., CHUNG, J. N., AND TROUTT, T. R., (2000), "*Experiments on particle dispersion in a plane wake". International Journal of Multiphase Flow*, **26,** 1583-1607.

